Modeling of Secondary System of SMART100 for Nuclear-Renewable Hybrid Energy System Analysis using MARS-KS

Jungjin Bang [a], Dong-Young Lee [a], Bub Dong Chung [a], Young Seok Bang [a], Youngsuk Bang [a], Seong-Su Jeon [a*]
[a]*Future and Challenge Tech., Gyeonggi-do, Yongin-si, Giheung-gu, Yeongdeok-dong, Heungdeok1ro, 13*
[*]*Corresponding author: ssjeon@fnctech.com*

1. Introduction

The main purpose of the Nuclear-Renewable Hybrid Energy System (NRHES) is to increase the efficiency and economy of power supply by combining nuclear power plants with renewable energy [1-2]. Particularly, nuclear power plants with high energy density can utilize as important energy source for various power systems. Also, it can compensate for the disadvantages of a nuclear power plant that cannot perform load following operation.

The NRHES can utilize an Electric Storage System (ESS) and a Thermal Energy Storage system (TES) to be used as a flexible resource facility to cope with the intermittency and volatility of energy demand of renewable energy as shown Figure 1. To make use of the TES, a portion of high temperature steam generated in nuclear power plants is extracted as thermal energy source. However, steam extraction can cause instantaneous transient that affects secondary system. Also, by providing thermal energy to the TES, the feedwater temperature is decreased, which may directly affect the core reactivity. Therefore, dynamic model for the secondary system analysis is essential to evaluate such transient conditions.

Prashant Sharma et al. [3] developed a dynamic model of secondary system of prototype fast breeder reactor to analyze the transient conditions such as feedwater pump trip event using RELAP 5 code. However, the analysis model excluded the components from the high-pressure turbine to the low-pressure turbine, i.e., it was not considered for variation of turbine power.

Dao-gang Lu et al. [4] set up the dynamic model of the secondary system for advanced PWR to evaluate the turbine load transient conditions using RELAP5 code. To simplify the model, all extraction pipes were modeled in boundary conditions. It is difficult to reflect the thermodynamic behavior in the extraction pipes in transient conditions.

In this paper, we developed the secondary system including turbines and extraction lines using MARS-KS code. To develop the analysis model, we used the heat balance diagram under Maximum Guaranteed Rate (MGR) condition in Standard Safety Analysis Report (SSAR) of SMART100. Furthermore, when the secondary system was combined with the TES, the variance of the turbine power cutback, thermal energy storage of TES, and inlet temperature of steam generators were analyzed according to operation conditions of TES.

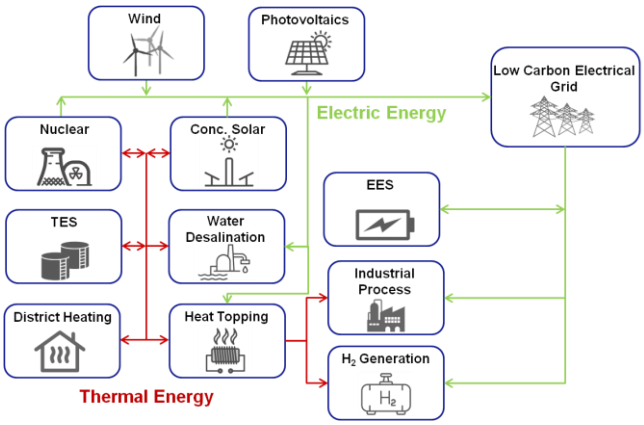

Figure 1. Conceptual design of the Nuclear-Renewable Hybrid Energy System

2. Secondary system model description

The secondary system for SMART 100 consists of steam generators (SGs), high-pressure turbine (HPT), moisture separator (SEP), re-heater (RH), low-pressure turbine (LPT), condenser (CD), condensate pump (COP), 4-stage low-pressure feedwater heaters (LFHs), Deaerator (DE), feedwater pump (FWP), and 2-stage high-pressure feedwater heaters (HFHs) as shown Figure 2.

2.1 Analysis model setup

The MARS nodalization for the secondary system of SMART100 is illustrated in Figure 3. In this paper, the secondary system was simplified by integrating feedwater heaters and extraction lines. For example, the four-stage LFH were integrated into one LFH (Tube side: 880, Shell side: 674), and the four extraction lines discharged low-pressure turbine to LFH were combined one extraction line (294). Therefore, it was modeled so that the total thermal energy of the four extraction lines and that of the combined extraction line were the same. Similarly, three-stage HFHs were combined into one HFH.

The steam generator was not modeled in the current phase. Instead, the temperature, pressure, and flow rate generated by SGs were modeled using time-dependent

volume (900) and time-dependent junction (095). The high-pressure turbine (210, 220, and 230) was modeled in three stages utilized turbine model built-in MARS code [5]. At each stage, the fluid was discharged into the re-heater, HFH, and deaerator to improve the efficiency of the secondary system, respectively. The moisture separator (260) was modeled using the SEPARATOR model built-in MARS-KS code [5]. The two-stage reheaters were integrated into one reheater (Tube side: 266, Shell side: 260). The low-pressure turbine was divided into 5 stages (280, 290, 300, 310, 320), and the steam of the 2nd stage was extracted into the LFH to increase the thermal efficiency. The condenser was modeled as two vertical pipes to prevent the thermal stratification inside the condenser, and a time-dependent volume (510) was used to control the pressure of the condenser. Also, the seawater circulation system for condensing the steam supplied to condenser was modeled using the time-dependent volumes (550, 560) and time-dependent junction (551). For COP and FWP modeling, the built-in Westinghouse pump model in MARS-code was used (710, 840). Deaerator was modeled with two vertical pipes for the same reason as the condenser.

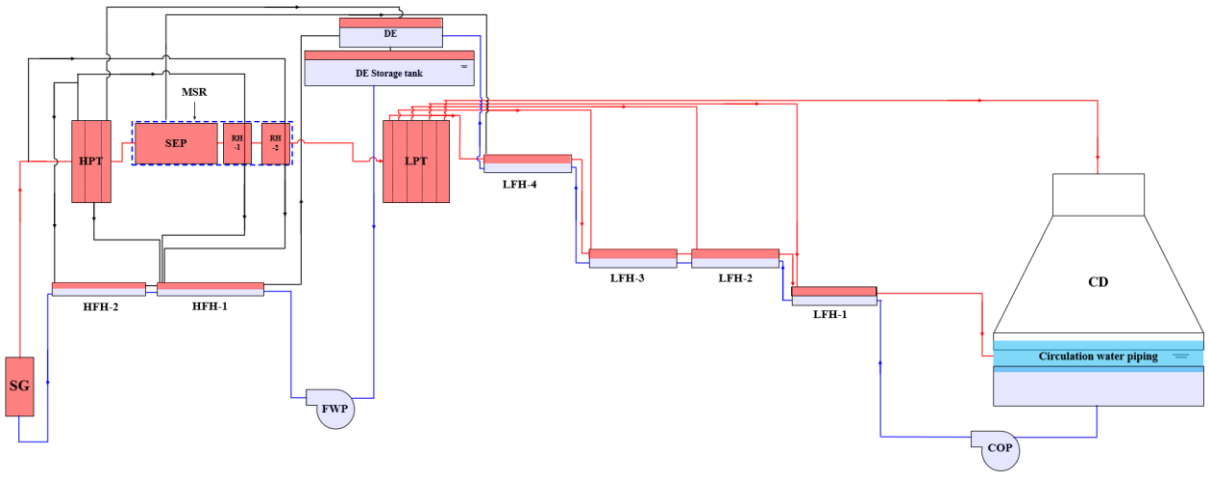

Figure 2. Schematic for the secondary system of the SMART100

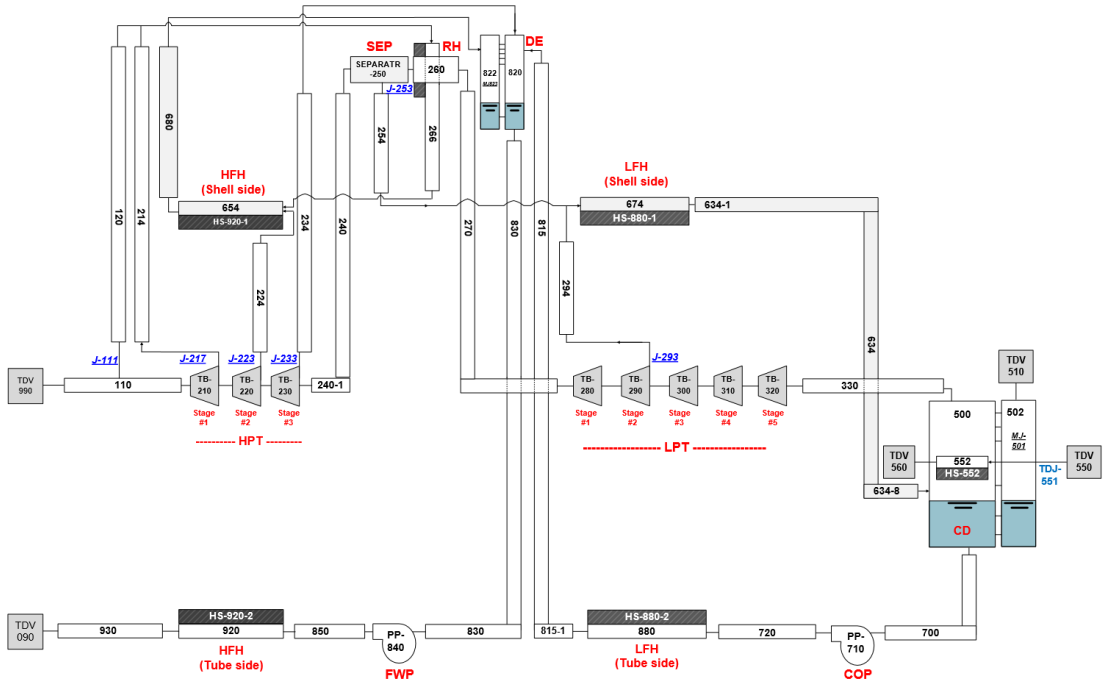

Figure 3. MARS-KS nodalization for the secondary system of SMART100

2.2 SPCS modeling validation

To validate the secondary system modeling, we compared the results obtained using MARS KS code with heat balance diagram at MGR in SSAR of SMAR100 [6].

Figure 4 shows the pressure behavior along with the main components, and the calculated results predict the behavior of the secondary system well. Figure 5 shows the temperature behavior in the main components. In general, the temperature behavior was predicted well, while the outlet temperature of heat exchangers such as the reheater, LFH was low. LFH has a complex design (e.g. drain cooling, condensing, and de-super heating zone) to increase the efficiency of the heat exchanger [7]. One of the main purposes of the LFH design is to properly separate condensed water from the steam supplied to the shell side and drain it to prevent insufficient or excessive accumulation of condensed water. This is because the water level of the heat exchanger can affect the vapor temperature of the shell side. However, the current LFH model was simplified to two horizontal pipes, thus, it was predicted that feedwater outlet temperature was low due to excessive accumulation of condensed water of the shell side. Accordingly, the heat exchanger modeling will be performed later using a 'multid' component model of MASR-KS to improve the heat exchanger model.

Figures 6 and 7 show the mass flow rate in the main and extraction lines, and the analysis results predict very well.

Based on the above results, it was confirmed that the secondary system of SMART100 was considered reasonable.

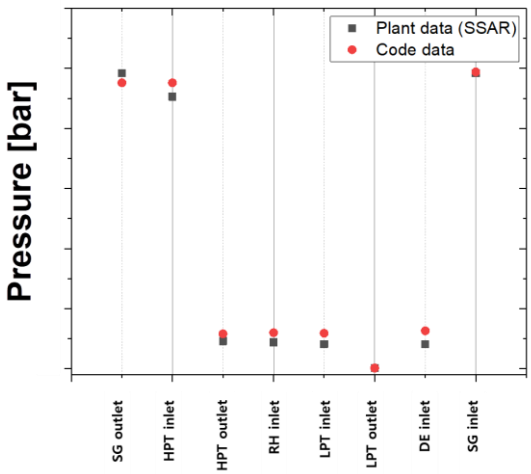

Figure 4. The pressure of main components

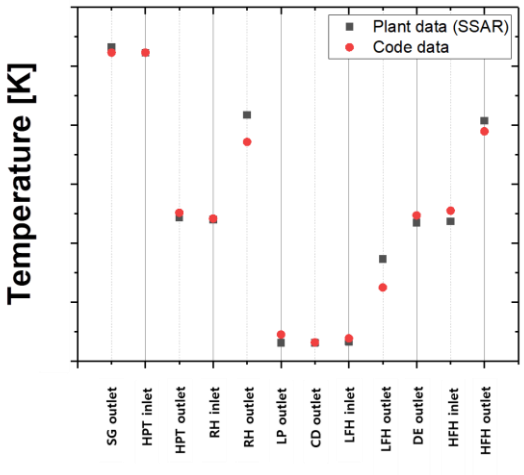

Figure 5. The temperature of the main components

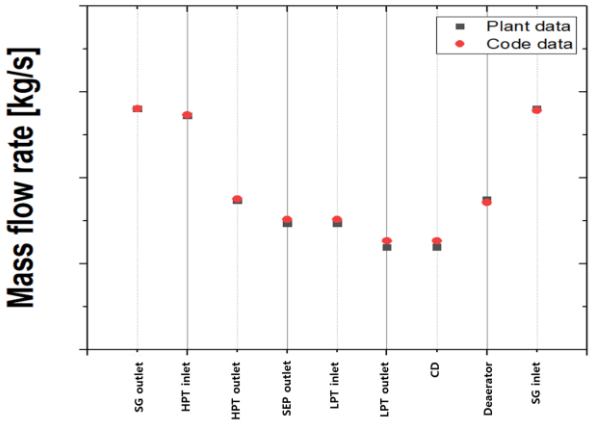

Figure 6. The mass flow rate of the main line

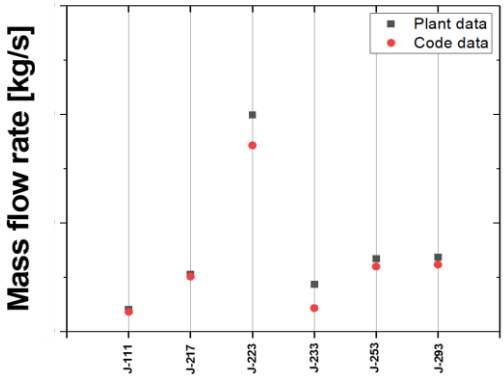

Figure 7. The mass flow rate of the extraction line

3. Analysis of the integration of the secondary system with thermal energy storage system

Figure 8 display the MARS code nodalization that integrates the secondary system and TES. The extraction flow rate is adjusted by the time-dependent

volume (50) and time-dependent junction (49) and the temperature and flow rate of the injection line are controlled using the time-dependent volume (54) and time-dependent junction (55). The extraction and injection positions are assumed to be the main steam line and deaerator, respectively. In this paper, a total of 9 cases are analyzed as shown in Table I.

Table I. Test cases for operation conditions of TES

Case	Extraction flow rate [kg/s]	Returned feedwater temperature [°C]
1	9.8	150
2		175
3		200
4	19.6	150
5		175
6		200
7	38.1	150
8		175
9		200

The analysis results can be seen in Figures 9 – 11. The lower the returned temperature, the lower the turbine power and Final Feedwater Temperature (FFT), i.e., the inlet temperature of SGs, although the heat storage of the TES increases. This is because when the returned temperature is lowered, the amount of steam required for the shell side of HFH increases. As a result, the turbine power is slightly decreased. However, since the amount of the total fluid flowing into the deaerator is relatively larger than that of TES, the FFT according to returned temperature is not significantly affected. On the other hand, an increase in the extraction mass flow rate has a large effect on the turbine power, heat storage rate of TES, FFT. Particularly, when the extraction flow rate is 38.1 kg/s, the FFT decreases by about 17 degrees Celsius compared to the normal operation conditions. Therefore, when designing the TES, it is important to select the extraction flow rate rather than the returned temperature.

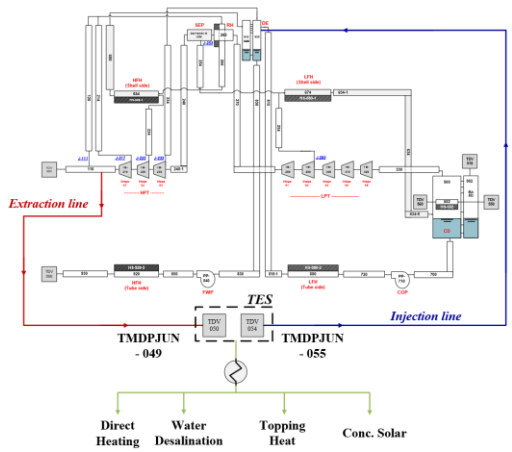

Figure 8. MARS-KS nodalization for the integration of secondary system with TES

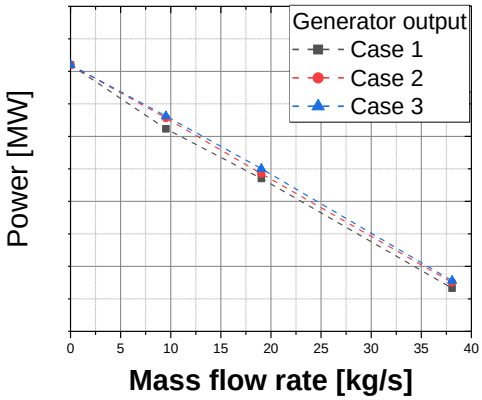

Figure 9. Turbine power according to extraction flow and return temperature

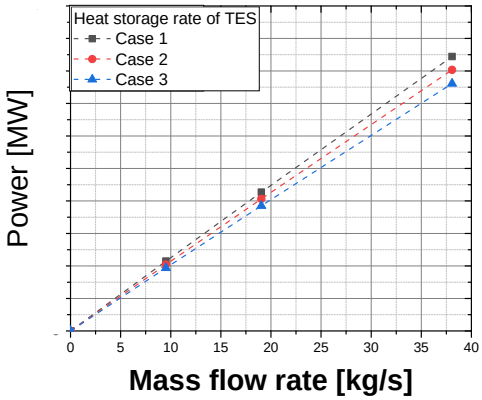

Figure 10. Heat storage rate of TES according to extraction flow and return temperature

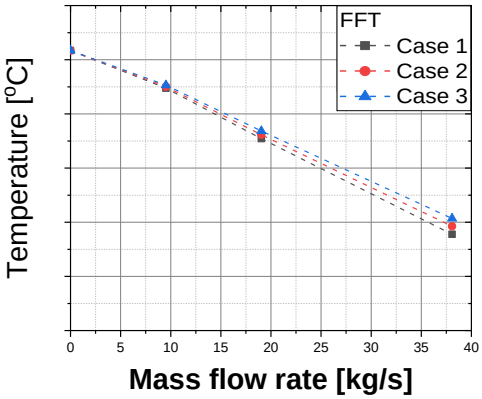

Figure 11. Final feedwater temperature according to extraction flow and return temperature

4. Conclusion and Future work

In this paper, the secondary system of SMART100 was modeled by using MARS-KS code, and it was confirmed that the analysis model predicted the thermodynamic behavior of the secondary system well.

In addition, we investigated the effect of TES operation on secondary system such as turbine power and inlet temperature of steam generator. As a result, the extraction flow rate had a significant effect on the secondary system rather than returned feedwater temperature. These results could be used as base data to analyze the dynamic behavior of the secondary system under operation conditions of TES.

Furthermore, dynamic behavior analysis for the optimal design of the TES (e.g., installation position of TES, extraction flowrate, returned temperature, etc.) will be performed by improving the developed model.

ACKNOWLEDGMENT

This work is supported by the Nuclear Research & Development program in the form of a National Research Foundation (NRF) grant funded by the Korean government Ministry of Trade, Industry, and Energy (No. 2021M2D1A1084837).

REFERENCES

[1] Ruth, M., Cutler, D., Flores-Espino, F., Stark, G., Jenkin, T., Simpkins, T., & Macknick, J. The economic potential of two nuclear-renewable hybrid energy systems, National Renewable Energy Lab, Golden, CO (United States), No. NREL/TP-6A50-66073, 2016

[2] Y. Bang et al, A Study on Flexibility Modeling of Nuclear-Renewable Hybrid Energy System, Transactions of the Korean Nuclear Society Autumn Meeting Goyang, Korea, October 24-25, 2019.

[3] Sharma, P., Natesan, K., Selvaraj, P., Balasubramaniyan, V., & Chellapandi, P., Dynamic modeling of steam water system of prototype fast breeder reactor using RELAP code. Annals of Nuclear Energy, *68*, 209-219, 2014.

[4] D. Lu et al, Full Scope Modeling and Analysis on the Secondary Circuit of Chinese Large-Capacity Advanced PWR Based on RELAP5 Code, Science and Technology of Nuclear Installations, Article ID 913274, 2015

[5] KINS, MARS-KS Code Manual, Volume II: Input Requirements, KINS/RR-1822, Vol. 2, Daejeon, Korea, 2018.7.

[6] KHNP, KAERI, KACARE, SMART100 Standard Safety Analysis Report, 2019.

[7] Heat Exchanger Institute Inc., Standards for Closed Feedwater Heaters, 9th Edition, 2015.